BRIEF REPORTS

Brief Reports are accounts of completed research which do not warrant regular articles or the priority handling given to Rapid Communications; however, the same standards of scientific quality apply. (Addenda are included in Brief Reports.) A Brief Report may be no longer than four printed pages and must be accompanied by an abstract. The same publication schedule as for regular articles is followed, and page proofs are sent to authors.

Stability of localized structures in the Swift-Hohenberg equation

Víctor J. Sánchez-Morcillo
Departament d'Òptica, Universitat de València, Dr. Moliner 50, E-46100 Burjassot, Spain

Kestutis Staliunas
Physikalisch Technische Bundesanstalt, Bundesallee 100, 38116 Braunschweig, Germany

(Received 28 April 1999)

We show that nonmonotonic (oscillatory) decay of the boundaries of phase domains is crucial for the stability of localized structures in systems described by Swift-Hohenberg equation. The less damped (more oscillatory) are the boundaries, the larger are the existence ranges of the localized structures. For very weakly damped spatial oscillations, higher-order localized structures are possible. [S1063-651X(99)07010-5]

PACS number(s): 64.60.Ak

In a previous paper [1] we analyzed the dynamics of phase domains in the real Swift-Hohenberg equation (SHE),

$$\partial_t A = A - A^3 - (\nabla^2 + \Delta)^2 A, \tag{1}$$

describing pattern formation in systems with a real order parameter $A(\mathbf{r})$ defined in two-dimensional (2D) space $\mathbf{r}=(x,y)$ and evolving in time t, and where $\nabla^2 = \partial^2/\partial x^2 + \partial^2/\partial y^2$. It has been shown that depending on the detuning Δ, a phase domain can contract, or expand. Contraction occurs for small values of detuning parameters ($\Delta < \sqrt{2/7} \approx 0.535$ as obtained analytically in [1], and $\Delta < 0.450 \pm 0.005$ as obtained numerically). For large values of detuning the domains expand leading to the ''labyrinth'' structures. For intermediate values of the detuning, the weakly contracting phase domains can stop contracting at a minimum radius, resulting in spatial localized structures (LSs).

These spatial LSs, being symmetric dark rings [rings of zero modulus of the order parameter $A(\mathbf{r})$], are characterized by a phase difference of π inside and outside of the ring. Predicted for SHE in [1], these LSs have been analyzed theoretically and numerically in degenerate optical parametric oscillators [2,3], and have been demonstrated experimentally in degenerate four-wave mixing [4]. Outside optics, these (or very similar) LSs were observed in periodically (parametrically) forced chemical systems [5]. These kinds of LSs are characteristic in every spatially extended system displaying supercritical pitchfork bifurcation, and are different from the LSs associated with subcritical bifurcations studied before in nonlinear optics and nonlinear physics [6].

Despite the above investigations [1–3], the mechanisms of stabilization of the supercritical LSs remain unclear. In [1] it was assumed that LSs are stabilized due to the balance of contraction of a circular domain boundary and the repulsion of the opposite segments of the dark ring. The stability of such LSs was investigated in [1] using a ''monotonic'' ansatz,

$$A_0(x) = \sqrt{1-\Delta^2}\tanh(x/x_0), \tag{2}$$

for the straight domain boundary directed along the y axis and with a half-width x_0, and also with the ansatz

$$A_0(r) = \sqrt{1-\Delta^2}\tanh[(r-r_0)/x_0]\tanh[(r+r_0)/x_0], \tag{3}$$

for a circular phase domain boundary with radius r_0. The analysis of the variational potential of SHE using the ansatz (3) yielded a potential minimum at some radius of the dark ring, predicting its stability, but the evaluated stability range ($0.39 \pm 0.01 < \Delta < 0.52 \pm 0.01$) differs from the numerically calculated stability range ($0.287 \pm 0.001 < \Delta < 0.460 \pm 0.001$). The ansatz (3) corresponds to the mutual repulsion of the opposite segments of the monotonically decaying dark ring.

The discrepancy between the numerically calculated LS existence range and that following from a ''monotonic'' ansatz (2) and (3) suggests that some other mechanisms are responsible for LS stability beyond that explored in [1]. We suggest in the present paper that a nonmonotonical decay of domain boundaries is essential for LS stability. We assume that the domain boundaries can be better described not by a monotonic function (2), but rather by an oscillatory function,

$$A(x) = \mathrm{sgn}(x)\sqrt{1-\Delta^2}\,[1 - e^{-\sigma|x|}\cos(kx)], \tag{4}$$

with a spatial decay rate σ and a spatial frequency k.

We show in this Brief Report that the nonmonotonic ansatz (4) leads to a perfect correspondence with the numerical results, thus justifying the role of nonmonotonic decay in the stability of LS. We show that the LSs stability range in-

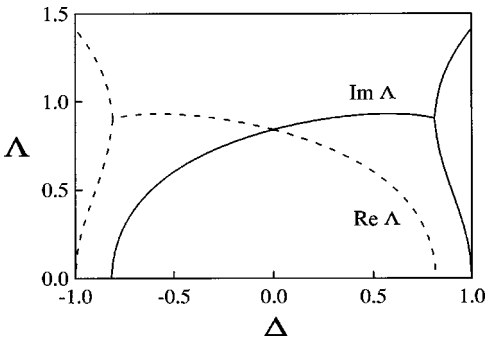

FIG. 1. The decay parameter $\sigma = \mathrm{Re}\,\Lambda$, and modulation wave number $k = \mathrm{Re}\,\Lambda$, depending on the detuning, as follows from the spatial stability analysis of SHE.

creases with increasing oscillations of nonmonotonical decaying fronts. We interpret in this way the fact that the LSs in degenerate optical parametric oscillators (DOPOs) are more stable than those in SHE: the oscillations of decaying fronts in DOPOs are indeed larger than in SHE. We also show that for very weakly damped spatial oscillations ($k/\sigma \gg 1$), higher-order localized structures are possible, such as rings with triple radius.

First we perform the spatial stability analysis of the stationary solutions of SHE in order to explore the decay of the spatial perturbation, and to determine the expected spatial decay σ and spatial frequency k. Boundary conditions, spatial inhomogeneities of some parameters, or the presence of a domain boundary (as a defect) can be considered as the spatial perturbation of homogeneous solution. The stationary solution $A_0 = \sqrt{1-\Delta^2}$ is thus perturbed,

$$A(x) = A_0 + \delta A e^{\Lambda x} + \text{c.c.}, \tag{5}$$

where Λ is in general a complex quantity, in the form $\Lambda = \sigma + ik$. The real part of Λ indicates the spatial decay of perturbation, while the imaginary part indicates whether there is a nonmonotonic decay.

In the spatial stability analysis the temporal derivative in Eq. (1) is set to zero. Inserting Eq. (5) into Eq. (1) and linearizing the resulting system with respect to perturbations, one obtains

$$\Lambda = \sigma + ik = \sqrt{-\Delta \pm \sqrt{3\Delta^2 - 2}}. \tag{6}$$

The dependence of σ and k on Δ following from Eq. (6) is given in Fig. 1.

In particular, $\mathrm{Re}\,q = 0$ for $\Delta = \sqrt{2/3}$. For larger values of detuning, only periodic solutions exist, which is in agreement with the usual temporal stability analysis of the homogeneous solution. For zero detuning $\sigma = k = 2^{1/4}$. For positive detuning the oscillations are more prominent than for negative detunings, as seen from Fig. 1. This is also in agreement with the fact that, for large negative detunings, the SHE can be reduced to a Ginzburg-Landau equation (GLE), in which is known the existence of monotonic solutions in the form (2) [7].

Motivated by these results of spatial stability analysis, we construct an ansatz for fronts with nonmonotonic decay (4). The ansatz (4), using the values of σ and k given by spatial stability analysis (6), and the profile of a domain boundary as

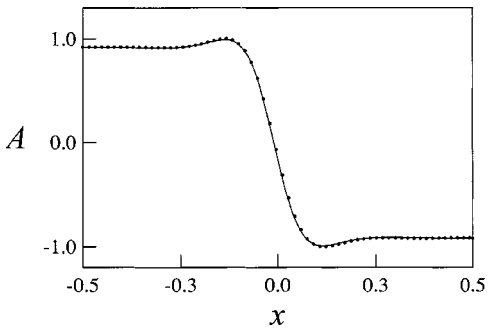

FIG. 2. Field profile around one-dimensional domain boundary. Dots corresponds to the result of numerical integration of SHE in 1D; the solid line corresponds to the ansatz (4) using the values of σ and k following from the spatial stability analysis. Detuning value is $\Delta = 0.4$.

obtained by numerical integration of SHE (1), are compared in Fig. 2. Note the good correspondence between both techniques.

Next we analyze the variational potential of SHE (1). Equation (1) can be written in the gradient form $\partial_t A = -\delta\mathcal{F}/\delta A$ with the potential $\mathcal{F}(A)$ given by [8]

$$\mathcal{F} = \int_{-\infty}^{\infty} \left[-\frac{A^2}{2} + \frac{A^4}{4} + \frac{[(\nabla^2 + \Delta)A]^2}{2} \right] d\mathbf{r}. \tag{7}$$

We use a variational approach in order (i) to determine the parameters σ and k in the ansatz (4) which minimizes the potential (3) in 1D, and (ii) to analyze the stability of LSs in 2D.

Due to the contribution of the homogeneous background A_0, an infinite value for the potential is obtained. Therefore we need to calibrate the potential (7) by subtracting this constant contribution [1–9], which in the 1D case yields

$$\mathcal{F} = \int_{-\infty}^{\infty} \left[-\frac{(A^2 - A_0^2)}{2} + \frac{(A^4 - A_0^4)}{4} + \frac{[(\partial^2/\partial x^2 + \Delta)A]^2}{2} - \frac{\Delta^2 A_0^2}{2} \right] dx. \tag{8}$$

Integration of Eq. (8) with ansatz (4) gives a value for the potential dependent on detuning Δ and on the parameters σ and k. The values of σ and k corresponding to the potential minimum are given in Fig. 3 as depending on the detuning.

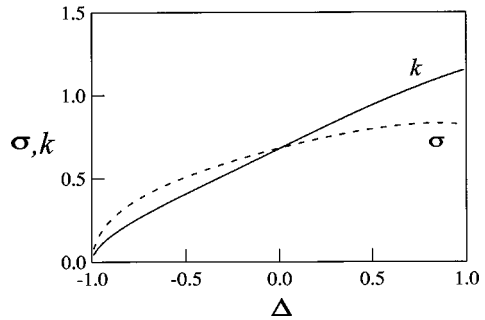

FIG. 3. The decay parameter σ and the modulation wavelength k depending on the detuning, as follows from the variational analysis of SHE (compare with Fig. 1).

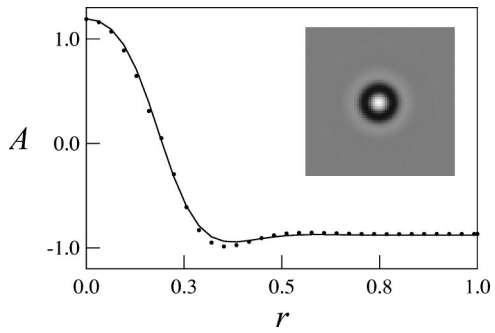

FIG. 4. Comparison of the LS profile in 2D, as obtained numerically (dots) and using the ansatz (8) (solid line). The profile of LS is taken at the line crossing the LS at its center. Detuning value is $\Delta = 0.4$. The inset shows the intensity distribution of the LS in the transverse plane.

Both following from spatial stability analysis (Fig. 1) or from variational analysis (Fig. 3), the oscillatory behavior is more prominent for increasing detuning: $\sigma < k$. For negative detuning $\sigma > k$, thus the oscillations are relatively strongly damped. However, the dependence on Δ shown in Fig. 1 and Fig. 3 differ one from another. Seemingly, the ansatz following from spatial stability analysis corresponds better for small perturbations (far away from the kink), and the ansatz following from the potential minimum corresponds better close to the core of the kink, where spatial perturbations are finite.

The calibrated potential (8) is positive in almost the whole detuning range, except for large detuning. The potential in 2D is equal to the potential in 1D multiplied by the length of the weakly curved domain boundary when the curvature effects are negligible in the potential [1]. Then, in this approximation, the sign of $\mathcal{F}_{1D}$ determines the evolution of the dark ring of large radius. For positive $\mathcal{F}_{1D}$ (small detuning) the large domains should contract, as the solution tends to minimize the potential. For detunings larger than some Δ_0, the 1D potential is negative, thus the domains should expand. As our calculations show, the equilibrium case occurs at detuning value $\Delta_0 \approx 0.462$, where the potential changes its sign. This equilibrium detuning value has been obtained using the values of σ and k following from the potential minimum (Fig. 3).

In a preceding paper [1] the critical detuning value was calculated using the monotonic ansatz. The obtained value $\Delta_0 = \sqrt{2/7} \approx 0.535$ differs from that obtained numerically $\Delta_0 = 0.450 \pm 0.005$. The critical detuning value using a nonmonotonic ansatz almost perfectly coincides with the numerical one when parameters are obtained by the potential minimum, and they are improved with respect to the monotonic case using parameters given by spatial stability analysis, where we found $\Delta_0 \approx 0.496$.

Next we analyze the stability of ring-shaped domain boundaries in 2D using the ansatz

$$A(r) = \mathrm{sgn}(r - r_0)\sqrt{1-\Delta^2}\,[1 - e^{-\sigma|r-r_0|}\cos(k(r-r_0))] \times [1 - e^{-\sigma(r+r_0)}\cos(k(r+r_0))], \quad (9)$$

where r_0 is the radius of the ring, and the decay parameters σ and k are given by 1D variational study. The ansatz (9) and the numerically calculated LS profile are compared in Fig. 4.

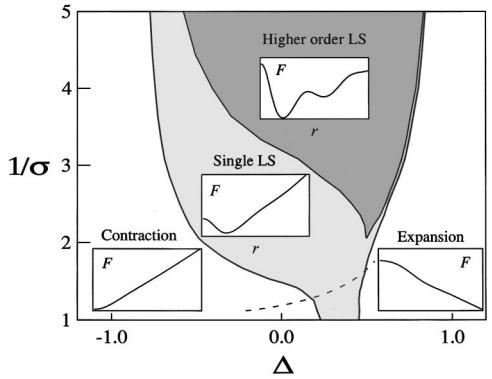

FIG. 5. The LSs existence range in the plane of $(1/\sigma, \Delta)$. The modulation wavelength k is given by the linear stability analysis (6); the decay parameter σ is chosen freely. The existence ranges of the single radius ring LSs and of the triple radius ring LS are plotted. The variational potential corresponding to all characteristic cases is shown in the insets.

The evaluation of potential (8) using the ansatz (9) yields the potential depending on the ring radius r_0. As predicted from the 1D calculations, for small (large) detunings, the potential monotonically increases (decreases) with the radius, leading to a contraction (expansion) of the ring. For some intermediate values of the detuning, the potential exhibits a minimum at some radius of the ring, as shown in the insets in Fig. 5. This potential minimum indicates the existence of localized structures.

As follows from variational analysis, the potential has a minimum for the detuning range $\Delta \in [\Delta_-, \Delta_+] = [0.27, 0.46]$. This range almost coincides with that obtained numerically, $0.287 \pm 0.001 < \Delta < 0.460 \pm 0.001$. Again we note that the existence range calculated in [1] by using the monotonic ansatz was much different from the numerical one.

Concluding, we show that the nonmonotonic decay of domain boundaries is essential for stabilization of the LS. The assumption of nonmonotonic decay allows us calculate precisely the critical detuning value for contraction-expansion of domains, as well as the existence range of localized solutions.

Next we explore how the LSs stability range depends on the modulation of the tails. For this purpose we assumed that the dynamics of domains is described by SHE (1), however that the modulation of domain boundaries is enhanced by some additional (perhaps nonvariational) effects. This occurs, e.g., in DOPOs. The domain dynamics is essentially governed by SHE, since SHE is the order parameter equation for DOPOs [10]. However, the presence of pump diffraction enhances the modulation of the fronts [11]. For this purpose we kept the value of k as follows from the spatial stability analysis of SHE [$k(\Delta)$ is a function of detuning], but varied arbitrarily the decay parameter σ. The approach is somewhat artificial, but it allows us to understand the role of oscillatory fronts in the stabilization of LS.

The result is plotted in Fig. 5. Clearly the LSs existence range grows with increasing oscillations of the decaying domain boundary (decreasing the parameter σ). The dashed curve corresponds to the decay rate σ calculated from the spatial stability analysis of SHE (6). The region above (be-

low) corresponds to spatial oscillations enhanced (damped) with respect to those in SHE. Then, for strong spatial oscillations the LS stability range significantly increases. This is in good correspondence with [2], where the LS stability range in DOPO was found to be larger than in SHE.

For sufficiently strong oscillations, the LS stability range extends even to the negative values of detuning. In [3], LS at zero detuning were predicted. Also, besides the fundamental LS (the ring of minimum radius $r_0 = r_{LS}$), higher-order LS may be stable, characterized by a set of discrete values of ring radius. The potential corresponding to a higher-order LS with $r_0 = 3r_{LS}$ is shown in the inset of Fig. 5. The structures with radius three times larger than the fundamental have been recently found numerically in DOPO in [3].

We acknowledge discussions with C.O. Weiss, G.J. de Valcárcel, and E. Roldán. This work has been supported by Acciones Integradas, NATO Grant No. HTECH.LG 970522, and by DGICYT of the Spanish Government under Grant No. PB95-0778-C02-01.

[1] K. Staliunas and V.J. Sánchez-Morcillo, Phys. Lett. A **241**, 28 (1998).

[2] K. Staliunas and V.J. Sánchez-Morcillo, Phys. Rev. A **57**, 1454 (1998).

[3] G-L. Oppo, A. J. Scroggie, and W. J. Firth, J. Opt. B: Quantum Semiclass, Opt, **1**, 133 (1999).

[4] V.B. Taranenko, K. Staliunas, and C.O. Weiss, Phys. Rev. Lett. **81**, 2236 (1998).

[5] V. Petrov, Q. Ouyang, and L. Swinney, Nature (London) **388**, 655 (1997).

[6] S. Fauve and O. Thual, Phys. Rev. Lett. **64**, 282 (1990); P. Mandel, M. Georgiou, and T. Erneux, Phys. Rev. A **47**, 4277 (1993); W.J. Firth and A.J. Scroggie, Europhys. Lett. **26**, 521 (1994); N. N. Rosanov, in *Progress in Optics*, edited by E. Wolf (North-Holland, Amsterdam, 1996), Vol. XXXV; S. Longhi, Phys. Scr. **56**, 611 (1997); G. Slekys, K. Staliunas, and C.O. Weiss, Opt. Commun. **149**, 113 (1998); K. Staliunas and V.J. Sánchez-Morcillo, *ibid*. **139**, 306 (1997).

[7] P. Manneville, *Dissipative Structures and Weak Turbulence* (Academic, San Diego, 1990).

[8] M.C. Cross and P.C. Hohenberg, Rev. Mod. Phys. **65**, 851 (1993).

[9] Y.S. Kivshar and X. Yang, Phys. Rev. E **49**, 1657 (1994).

[10] K. Staliunas, J. Mod. Opt. **42**, 1261 (1995); G.J. de Valcárcel, K. Staliunas, E. Roldán, and V.J. Sánchez-Morcillo, Phys. Rev. A **54**, 1609 (1996).

[11] K. Staliunas and V.J. Sánchez-Morcillo (unpublished).